Active Flux Based Advanced Encoderless AC Drives: A Tutorial Review

Ion Boldea, *Life Fellow, IEEE*, Ana-Adela Popa, *Member, IEEE*, and Frede Blaabjerg, *Fellow, IEEE*

***Abstract*—"Active flux" is an alternative unitary concept for the control of practically all ac drives. As aligned to rotor *d*-axis (for synchronous and flux-modulation machines) and to rotor flux axis for induction machines, "active flux" is a physical/technical concept that turns all travelling field physically salient electric ac machines into a functionally nonsalient model. As its position is independent of load torque (for known machine parameters) it leads to notable simplifications in encoderless advanced control of ac drives. This tutorial review summarizes the fundamentals of the "active flux" concept as applied to practically all ac machines and the progress from 2008 to today with sample literature results. It also introduces in draft the theory of applying "active flux" to MTPA, MaxCosFi, maximum torque per flux (MTPF) integrated into smooth control of ac drives, for constant and variable magnetic saturation, with promising recent results for a reluctance synchronous motor drive. Weighting "active flux" merits and demerits and offering new workfronts in its application the article is hoped to assist in producing even better ac motor/generator drives in the future.**

***Index Terms*—AC drives, "active flux", encoderless control systems, maximumCos*Fi*, maximum torque per ampere (MTPA), maximum torque per flux (MTPF).**

NOMENCLATURE

E	Extended EMF.
L_d, L_q	*dq* inductances of synchronous motors.
Ψ_{PM}	PM flux linkage.
T_{ePMSM},T_{eEESM}, T_{eRSM},T_{eIM}	Electromagnetic torque of permanent. magnet synchronous motor (PMSM), electrically excited synchronous motor (EESM), reluctance synchronous motor (RSM), and induction motor (IM).
$\Psi^a_{d\text{PMSM}}$,$\Psi^a_{d\text{EESM}}$, $\Psi^a_{d\text{RSM}}$, $\Psi^a_{d\text{IM}}$	Active flux linkage vectors of respective motors defined above.
L_s, L_{sc}	No load and short-circuit inductance of IM.
$\omega_{r\text{IM}}$	Electric angular rotor speed of IM.
$S\omega_1$	Slip angular frequency of IM.
R_s, $\overline{V}_s$, $\overline{I}_s$	Stator phase resistance, stator voltage, and current space vectors.
s	Laplace operator.
$\overline{\Psi}_s$	Stator flux linkage space vector.
PLL	Phase locked-loop.
θ_{er}	rotor d axis position with respect to stator phase "a."
i_d, i_q	*dq* stator currents.
ALA rotor	Axially laminated anisotropic rotor ($L_d>>L_q$).
Ψ_{F0}	Electric excitation flux linkage amplitude.

Manuscript received 10 October 2023; revised 15 January 2024 and 25 March 2024; accepted 17 May 2024. Date of publication 24 May 2024; date of current version 4 September 2024. Recommended for publication by Associate Editor S. Yang. *(Corresponding author: Ana-Adela Popa.)*

Ion Boldea and Ana-Adela Popa are with the Electrical Engineering Department, Politehnica University Timisoara, 300223 Timişoara, România, and also with Romanian Academy, 300223 Timişoara, România (e-mail: ion.boldea@upt.ro; ana.popa@upt.ro).

Frede Blaabjerg is with the AAU Energy, Aalborg University, 9220 Aalborg, Denmark (e-mail: fbl@energy.aau.dk).

Color versions of one or more figures in this article are available at https://doi.org/10.1109/TPEL.2024.3405073.

Digital Object Identifier 10.1109/TPEL.2024.3405073

I. INTRODUCTION

CONVENTIONALLY signal injection (SI) or (and) fundamental model (FM) based encoderless control systems for ac drives-field oriented control (FOC) [1], [2], direct torque and flux control (DTFC) [3], feedback linearization control (FL) [4] and model (or model-free) predictive control (MPC) [5]—process current vector or inductance or EMF in observers to detect simultaneously rotor (or rotor flux for IM) position and rotor speed, from zero to maximum speed, but strong filtering introduces delays. These delays have been alleviated in many ways, but the control became inevitably more complicated, especially by introducing operation modes such as maximum torque per ampere (MTPA), MaximumCos*Fi* and maximum torque per flux (MTPF), to increase performance and torque–speed range within limited dc input voltage of the inverter that feeds the ac motor/generators.

The alternative would be to "observe" the "flux" and to process it directly to yield/estimate rotor position and speed. But this approach was considered problematic until the offset related to integrals etc. was alleviated by the introduction of second order generalized integrals [SOGI or reduced order generalized differentiators (ROGD)] etc. [6].

As the stator flux with respect to rotor (or rotor flux) axis vector position varies with load (even with constant machine parameters), and thus its speed $\omega_{\Psi s}$ is equal to rotor speed (for SMs) only during steady state, other candidates were looked for, in order to simplify the combined rotor position and speed observer in advanced encoderless ac drives.

One of the first attempts was made with "extended EMF" [1] of interior permanent magnet synchronous machine (IPMSM)

$$\overline{E} = ((L_d - L_q)\cdot i_d + \Psi_{\text{PM}})\cdot\omega_1 + j\cdot\omega_1 L_q \frac{di_q}{dt} \quad (1)$$

which managed to somewhat reduce the complexity of rotor and speed observation. Next step was to use the first term in (1) but only as a virtual flux of IPMSM [7]

$$\Psi_{\text{virtual}} = (L_d - L_q) \cdot i_d + \Psi_{\text{PM}} \tag{2}$$

where L_d, L_q are the *dq* axes inductances.

The "virtual flux" concept in [7] for IPMSM was generalized for all ac machine drives as "active flux" $\overline{\Psi}_d^a$ (it is called "active flux" as it contributes to the total torque of all ac (traveling field) motor/generator drives), starting from torque expression scrutiny [8]

$$\begin{aligned}
T_{e\text{PMSM}} &= \frac{3}{2} p_1 \left((L_d - L_q) \cdot i_d + \Psi_{\text{PM}} \right) \cdot i_q && \text{for IPMSM in rotor coordinates} \\
&= \frac{3}{2} p_1 \Psi^a_{d\text{PMSM}} \cdot i_q; \\
T_{e\text{EESM}} &= \frac{3}{2} p_1 \left((L_d - L_q) \cdot i_d + L_{dm} \cdot i_F \right) \cdot i_q && \text{for EESM in rotor coordinates} \\
&= \frac{3}{2} p_1 \Psi^a_{d\text{EESM}} \cdot i_q; \\
T_{e\text{RSM}} &= \frac{3}{2} p_1 \left(L_d - L_q \right) \cdot i_d \times i_q && \text{for EESM in rotor coordinates} \\
&= \frac{3}{2} p_1 \Psi^a_{d\text{RSM}} \cdot i_q \\
T_{e\text{IM}} &= \frac{3}{2} p_1 \left(L_s - L_{sc} \right) \cdot i_d \cdot i_q && \text{for IM in rotor flux coordinates} \\
&= \frac{3}{2} p_1 \Psi^a_{d\text{IM}} \cdot i_q
\end{aligned} \tag{3}$$

where L_s, L_{sc}—no load and short-circuit induction machine (IM) inductances and i_F—field current

As noticed in (3) the "active flux" is aligned to *d*-axis (of *dq* model) if the machine parameters are known, indifferent of torque (load)—and thus the speed of the "active flux" is rotor speed in synchronous (and flux-modulation) machine drives and it is the rotor-flux speed for the IM, $\omega_{\Psi r}$.

Thus, for IMs the rotor speed $\omega_{r\text{IM}}$ is:

$$\omega_{r\text{IM}} = \omega_{\Psi^a_{d\text{IM}}} - \quad S \cdot \omega_1, \text{ where} - \text{slip frequency}. \tag{4}$$

For synchronous and flux—modulation—machine drives:

$$\omega_r = \omega_{\Psi^a_d} \tag{5}$$

Note: Flux-modulation ac machines produce torque through the fundamental and a few harmonics of stator mmf due to their special topology [9] essentially could be considered as synchronous machine.

And it is, in general, obtained through a phase-locked loop (PLL) on the estimated rotor position $\widehat{\theta}_{\Psi^a_d}$, which will yield a better rotor position via $\widehat{\theta}_{\Psi^a_d}$ and its speed $\widehat{\omega}_{\Psi^a_d}$, though still speed estimation "inherits" the position estimation error inevitably.

Note: For surface permanent magnet synchronous machines (SPMSMs) ($L_d = L_q = L_s$) the "active flux" coincides with rotor (PM) flux Ψ_{PM}.

It should be noted that apparently the "active flux" turns machines with physical "magnetic saliency" into functionally nonsalient machine(s) model, which should be characterized by a single inductance L_q. If so, then, we consider again the *dq* model of ac machines

$$\overline{I}_s R_s - \overline{V}_s = -\frac{d\overline{\Psi}_s}{dt} - j \cdot \omega_r \, (or \ \omega_{r\text{IM}}) \cdot \overline{\Psi}_s \quad \text{with} \tag{6}$$

$$\overline{\Psi}^a_d = \overline{\Psi}_s - \overline{I}_s L_q. \tag{7}$$

We obtain

$$\begin{aligned}
\overline{I}_s R_s - \overline{V}_s = & - \frac{d\Psi^a_d}{dt} - j \cdot \omega_r \, (or \ \ \omega_{rIM}) \\
& \cdot \Psi^a_d - L_q \frac{d\overline{I}_s}{dt} - j \cdot \omega_r L_q \overline{I}_s \\
= & - (j \cdot \omega_r + s) \, L_q \overline{I}_s - (j \cdot \omega_r + s) \, \bar{\Psi}^a_d.
\end{aligned} \tag{8}$$

This vector (8) reflects the presumption that, in "active flux" terms, the ac machines manifest themselves as nonsalient machines in the *dq*-model, with a single inductance, L_q, while "active flux" position is rotor position (axis *d* here) for synchronous and flux-modulation machines and it is rotor flux position in IMs, indifferent of torque (load) value, in any coordinate system and at any speed; for injection signal or for FM.

Note: On Fig. 1(c) related to PM assisted reluctance synchronous machines (RSMs)—the PM axis is still kept in axis d (L_d<L_q), but we could simply apply the "active flux" concept swapping the *d–q* axis as for the RSM (no PMs) in Fig. 3(d).

Based on (8) we may simply state that the "active flux model" with axis *d* along rotor axis (in synchronous machines and in rotor flux axis in IMs) represents phenomenologically the respective machines. The "active flux" is thus a technical not only a mathematical concept.

Note: It goes without saying that inverter nonlinearities, magnetic saturation and parameters detuning causes a departure of "active flux" axis (position) estimation from reality, as it did in the stator (rotor) flux observers and, consequently, should be corrected.

Let us notice that L_q in wound rotor synchronous machines (WRSM) and ALA-rotor reluctance synchronous motor (RSM) (or L_{sc} for IMs) in (3) is weakly dependent on saturation but not so in IPMSM (with L_q>L_d, Fig. 3(c) and (d) and dependent on magnetic saturation).

An illustration of the "active flux" concept in permanent magnet synchronous machines (PMSMs), WRSMs, RSMs, and IMs *dq* models in *dq* coordinates as discussed above, is shown in Fig. 1.

A. *"Active Flux" Merits*

1) Turning magnetically (or virtually as in IM in rotor flux coordinates) salient rotor synchronous, flux modulation and IMs into nonsalient *dq* models, "active flux" concept simplifies rotor position and speed observers by the fact that "active flux vector" has rotor d axis (or rotor flux

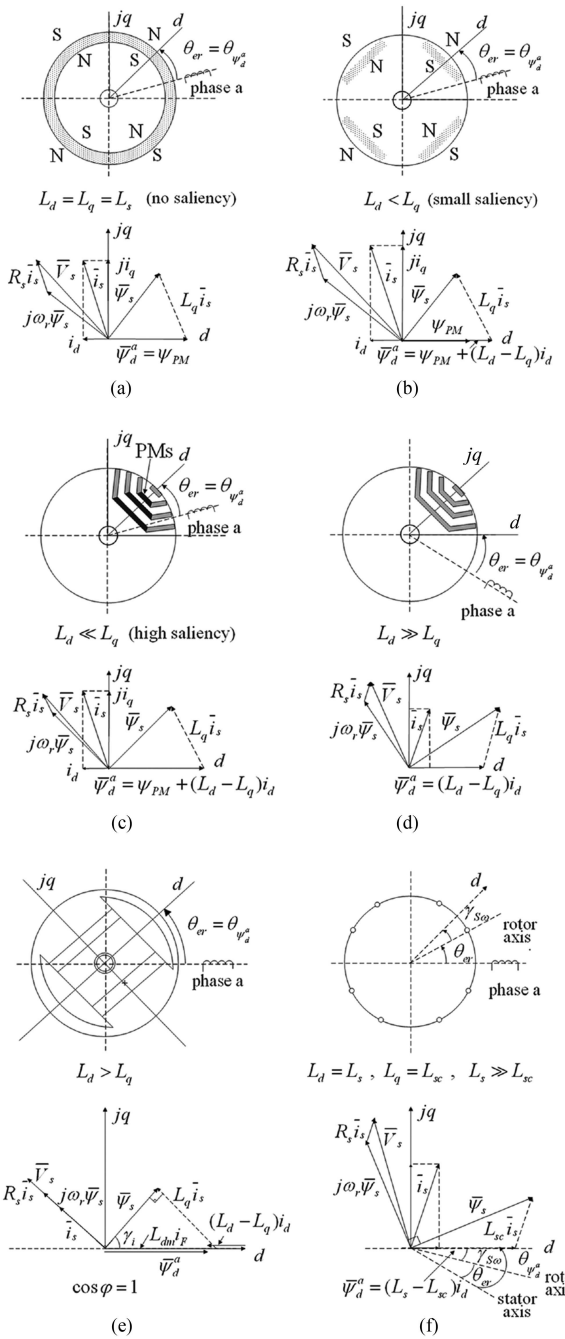

Fig. 1. "Active flux" illustration in the *dq* models of: (a) surface permanent magnet synchronous machine; (b) and (c) interior permanent magnet synchronous machines; (d) Relsyn; (e) DC-excited SM; and (f) induction machine, after [8].

in IMs) orientation indifferent of the load (torque) value, in contrast to stator flux. It applies to all travelling field electric motor/generator drives.

2) "Active flux" concept allows rotor and position observation also for SI state observer even at zero speed if physical magnetic saliency exists; including initial position with PM (or dc excitation) flux polarity.
3) The use of SOGI-like schemes allows efficient "active flux" direct processing to observe rotor position and speed [6].
4) The above simplifications were already acknowledged in [8] and have been enriched subsequently since 2008 in numerous publications [9], [10], [11], [12], [13], [14], [15], [16], [17], [18], [19], [20], [21], [22], [23], [24], [25], [26], [27], [28], [29], [30], [31], [32], [33], [34], [35], [36], [37], [38], [39], [40], [41], [42], [43], [44], [45], [46], [47], [48], [49], [50], [51], [52], [53], [54], [55], [56], [57], [58], [59], [60], [61], [62], [63].
5) In this article, besides summarizing recent progress on "active flux" implementation, we add the derivation of MTPA, MaxcosFi, MTPF conditions using "active flux" for all ac machine drives (with a case study for axially laminated anisotropic reluctance synchronous motors), without and with magnetic saturation considered in the derivations, from the beginning.
6) The "active flux" concept may be extended to linear induction and synchronous motor/generators control, replacing torque for thrust and rotary speed for linear speed and "adding" the longitudinal end effects by disturbance observers.

B. *"Active Flux" Challenges/Demerits*

1) As already mentioned, "magnetic saturation" also causes an error in "active flux" position observation if we use constant machine parameters (as it did for other flux vector choices: stator flux; rotor flux; and airgap flux). So, corrections for parameter detuning are required for precise fast torque response of electric drives.
2) The machine parameters may be online estimated and corrected or treated together with inverter nonlinearities, inertia, load torque variation as disturbances, to be online estimated and added to the "active flux" observer [10] to reduce position and speed coupling [57] estimation errors.
3) However, it should be noted that so far only the "active flux" position and speed were observed while its amplitude, especially with $Lq \approx$const (as in WRSM, SPMSM, ALA-rotor RSMs, IMs), is still available from the "active flux" observer for direct online correction of one machine parameter (*Ld* or *Ldm*).
4) Varatharajan and Pellegrino [41] developed on "active flux" produced position and speed observation to preserve stability at overload for a RSM drive.
5) MaxCosFi was added as a distinct operation mode as its stator flux for given torque is between MTPA and MTPF (as shown later in this article) and all three operation modes are independent of speed for given machine parameters and losses are neglected. The losses lead to a decrease of efficiency but to an increase in actual power factor. MaxCosFi operation mode is mainly useful to base speed for more torque (power) for wide constant power speed range (CPSR) in RSM and IMs which have high physical saliency [$Ld >> Lq$ (RSM), $Ls >> Lsc$ (IM)].

So, this article continues as follows.

1) State of the art on "active flux" in ac drives control in Section II like: IPMSMs; RSMs; IMs; dc excited machines; flux–modulation (F–M) machines.

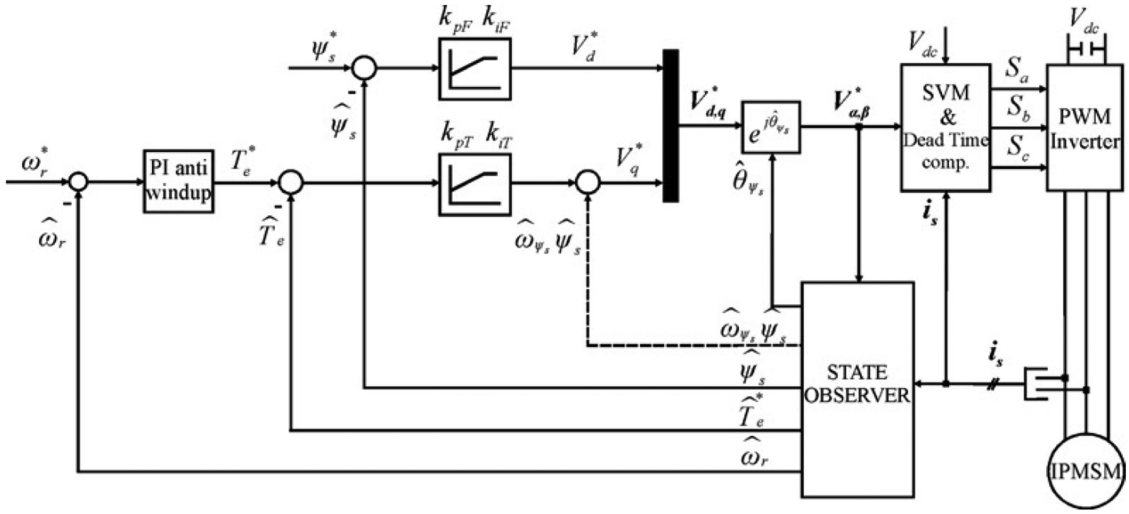

(a)

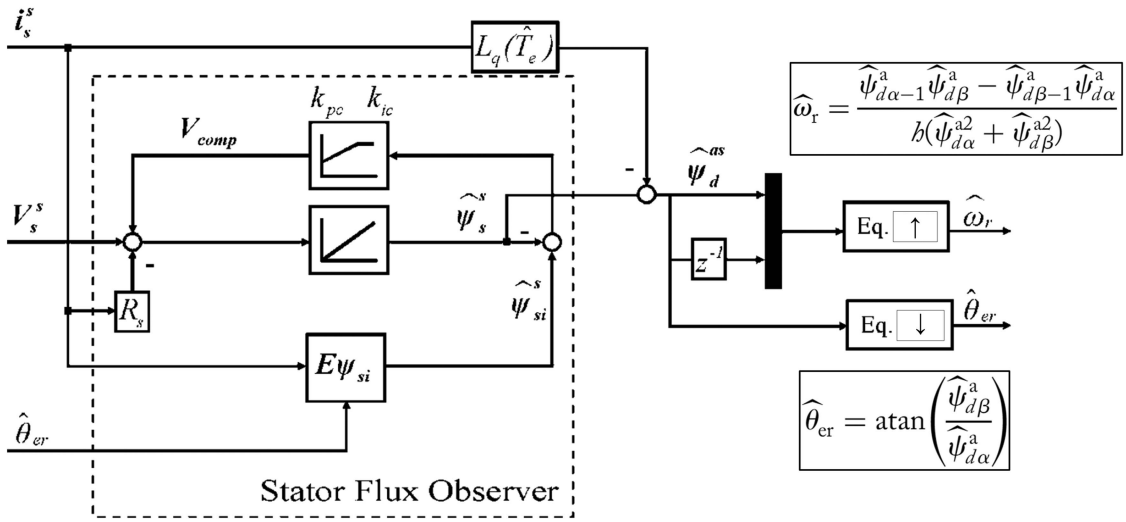

(b)

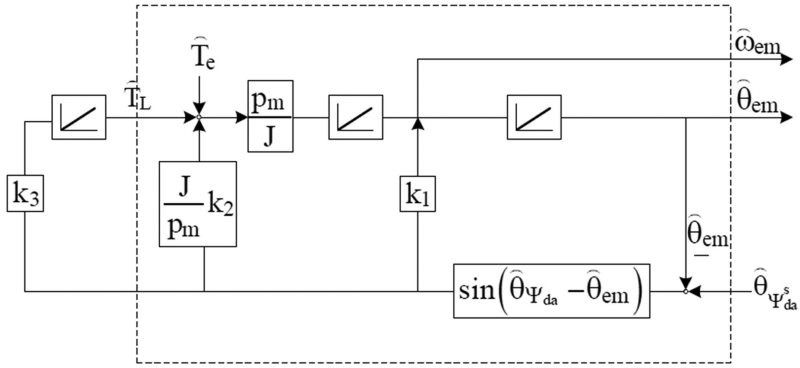

(c)

Fig. 2. Control systems. (a) Generic encoderless DTFC control system for PMSM. (b) and (c) Typical voltage plus current model close loop active flux observer with PLL for PMSMs, IMs, and RSMs [12].

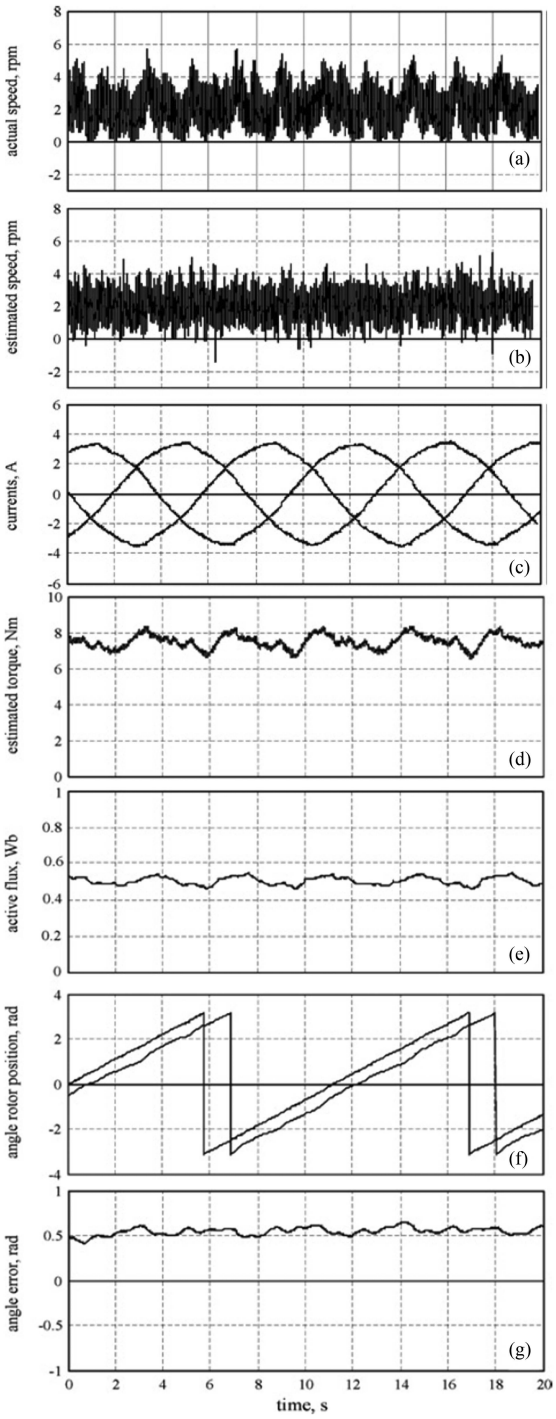

Fig. 3. Vector control: steady state encoderless operation at lowest speed of 2 r/min (0.1 Hz) and 50% rated torque. (a) Actual speed. (b) Estimated speed. (c) Measured currents. (d) Estimated torque. (e) Active flux. (f) Actual and estimated rotor position. (g) Rotor position error [11].

2) Extension of "active flux" concept to MTPA, MaxCosFi, MTPF wide torque-speed control without and with magnetic saturation from start, with sample results on an ALA RSM drive, with experiments in Section III.
3) Discussion and conclusions in Section IV.

II. State of the Art on "Active Flux" in AC Machine Drives

A. Fundamental "Active Flux"

The key to the encoderless "active flux" FM is the "active flux" observer, which should be rather similar for all ac drives, if a notable simplification of control technology is targeted.

A main competitor in this sense proved to be the combined closed-loop voltage plus current model for stator flux $\widehat{\Psi}_s$ with subtracted $I_s L_q$ followed by a PLL to improve its precision on both estimated angle $\widehat{\theta}_{\Psi_d^a}$ and estimated speed $\widehat{\omega}_r$ (see Fig. 2). The PI closed loop controllers in the observers may be complemented for robustness, by sliding mode components.

The PLL may include the motion equation, to secure good precision for speed estimation under load torque fast perturbations during speed transients (see Fig. 2(b) and (c) [12]).

Note: The amplitude of $\widehat{\Psi}_d^a$ estimation, which is available as a bonus, may be "exploited" to correct online one machine parameter (L_d or $L_{\rm dm}$ or $\Psi_{\rm PM}$) which varies most due to magnetic saturation or/and temperature.

The "active flux" observer may simply be included in FOC, DTFC, feedback linearization, MPC encoderless controls [11] with added disturbance observers for more robust control responses.

Subsequently, numerous papers have improved/developed/implemented [17], [18], [19], [20], [21] concepts of similar or equivalent "active flux" under the "name" of "virtual flux," "extended flux," "equivalent flux" [13], "rotor flux model" [14], "fictitious flux" [15], "auxiliary flux" [16], many inspired from the extended EMF concept [1].

Also, recent implementations to IPMSM drives using sliding mode "active flux" (some with a disturbance) observer [22], [23], [24], [25], [26], [27], [28], [29], [30], [31], [32] have been introduced to enhance the robustness to machine parameters and load torque perturbations and to reduce the lowest speed operation, under full step torque perturbation down to 2 r/min proven in experiments [12], see Figs. 3 and 4.

The so far mentioned literature is referring mainly to PMSM drives (IPMSM, mostly), but very recently it was also applied to RSM encoderless control [with $\Psi_{\rm PM} = 0$ and $L_d > L_q$ in contrast to IPMSM ($\Psi_{\rm PM} \neq 0$ and $L_d \neq L_q$)] which, in terms of fundamental "active flux" concept, is discussed in [34], [35], [36], [37], [38], [39], [40], [41], [42], and [43]. An example of I–f for starting, combined with FOC active-flux-based encoderless control of RSM [34] is presented in Fig. 5. The difference between measured and estimated rotor position during I–f to FOC transition [see Fig. 5(b)] is to be expected. However, Fig. 5(c) shows stable speed response over a large speed range.

Only a few attempts to use "active flux" for MTPA in IPMSM and RSM encoderless drives [44], [45], all without considering magnetic saturation, have been made so far, despite possible simplifications.

Also, advanced scalar encoderless control (V/f and I–f control methods)—with stabilizing loops—for IPMSMs, IMs, and RSMs based on "active flux" have been recently proposed, especially for maximum power factor, to yield a better wide

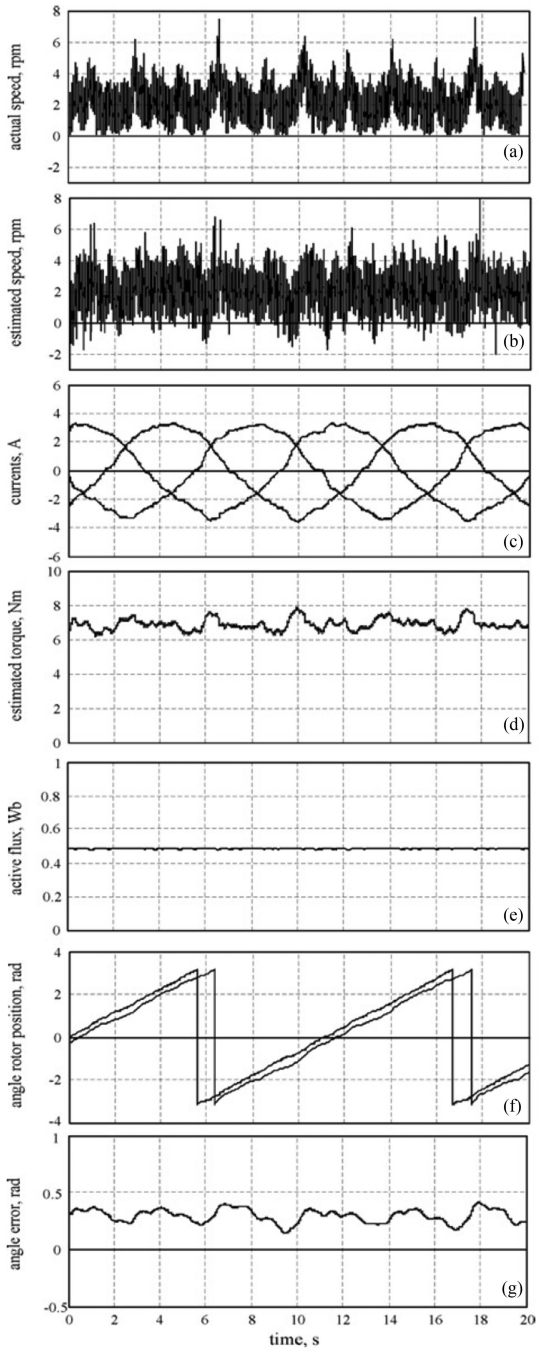

Fig. 4. DTFC: steady state encoderless operation at lowest speed of 2 r/min (0.1 Hz) and 50% rated torque. (a) Actual speed. (b) Estimated speed. (c) Measured currents. (d) Estimated torque. (e) Active flux. (f) Actual and estimated rotor position. (g) Rotor position error [11].

speed range energy conversion [46], [47], [48], [49], as, again, notable simplifications in the implementation have been found and providing rather close to FOC and DTFC performance in control (see Fig. 6).

B. Case of Fundamental "Active Flux" Concept in Encoderless Electrically Excited SM Drives

As alluded to in Introduction the "active flux" in dc excited (and given field current) SMs is similar to the one in IPMSM but

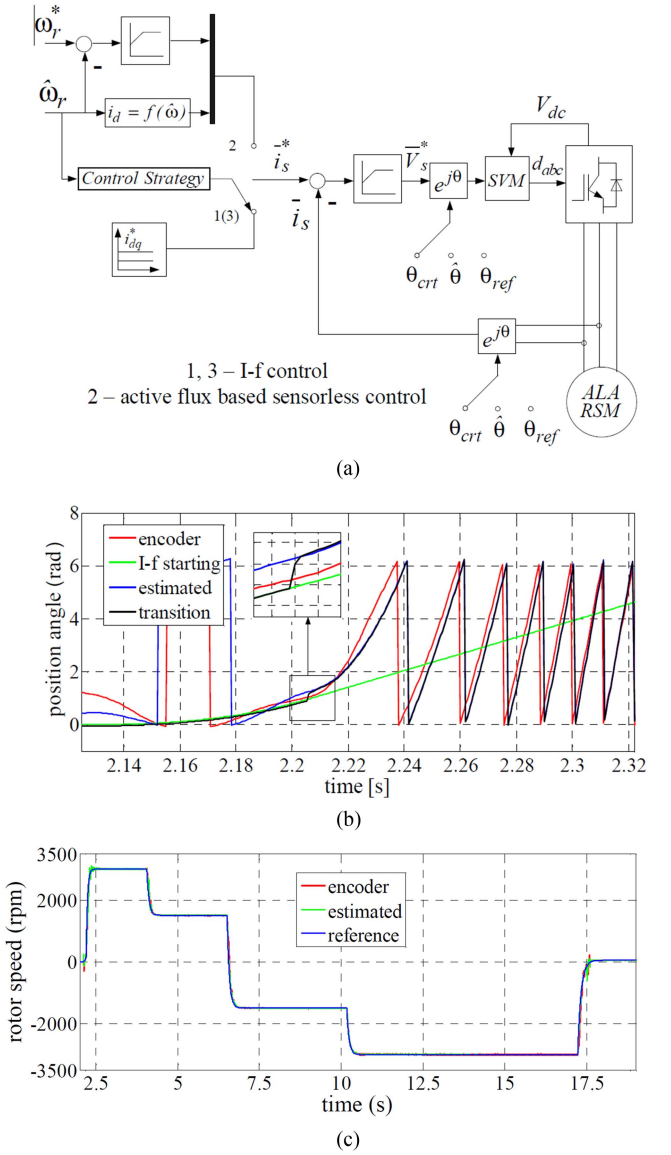

Fig. 5. I–f plus active flux encoderless RSM control. (a) Control scheme. (b) Sample transition transients. (c) Wide speed range control, [34].

with $L_d > L_q$ (normal saliency) [50], [51]. In drives where below 10–15 r/min heavy load operation is not required, it suffices to estimate the initial rotor position by injecting a dc voltage pulse in the field winding with the inverter short-circuited (zero voltage vector) and record i_α, i_β and notice that the d-axis is opposite to the stator currents mmf position [50], (see Fig. 7).

Also, in electrically excited SMs there is one more variable i_F (field current), that is open to change for energy conversion optimization, say, for $i_d = 0$ control during acceleration, below base speed, and unity power factor above base speed, to max speed, in wide CPSR) applications. Such an encorderless drive has been started on full friction (load) torque—80 N·m—(from zero speed) (see Fig. 7, [50]).

The "active flux" observer (considering here cross-coupling saturation estimation online) for this drive is shown in Fig. 8(a)–(c).

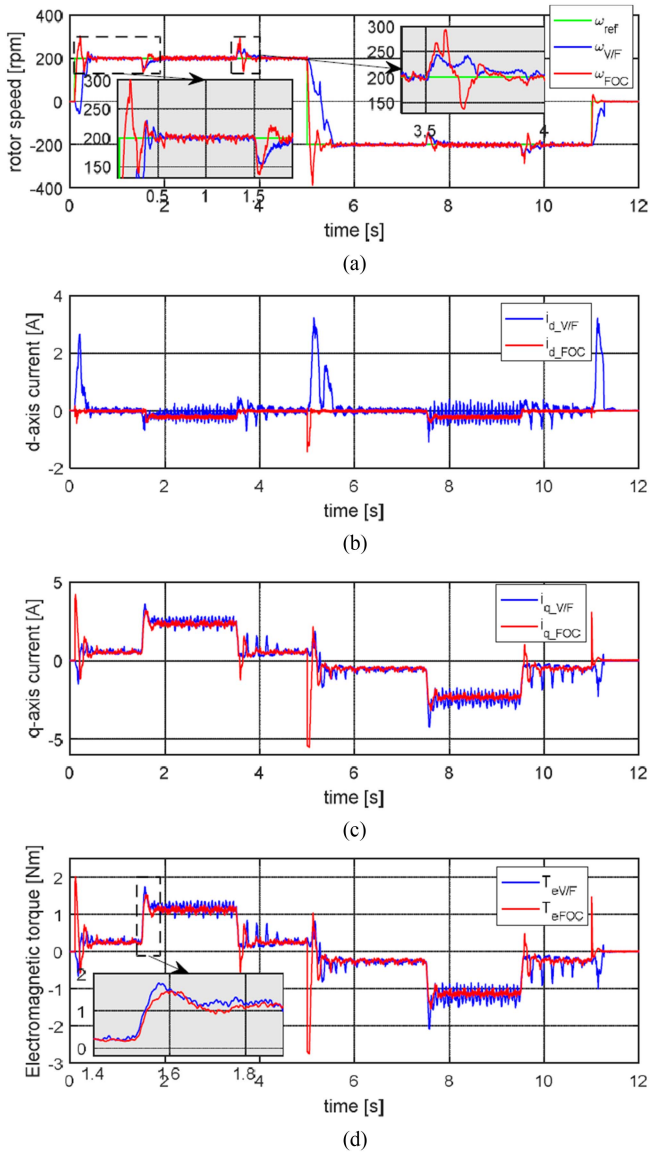

Fig. 6. Encoderless V/f control with stabilizing loops versus FOC at ±200 r/min reference speed under load torque transients. (a) Reference and estimated speed. (b) Estimated d current. (c) Estimated q current. (d) Estimated torque [46].

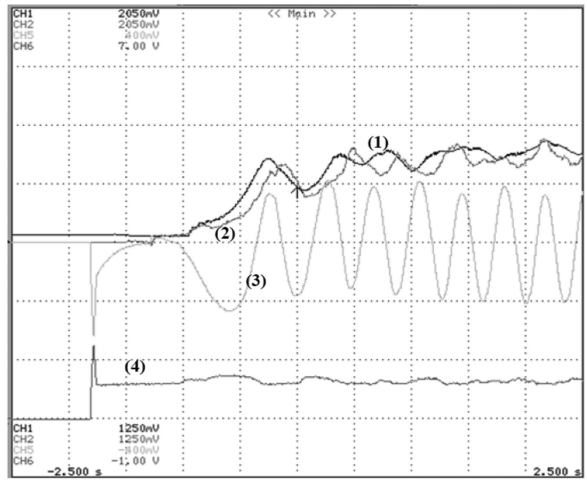

Fig. 7. Electrically excited SM, initial rotor position searching, and start to 80 r/min, 100% load. (1) Estimated and (2) measured speed (10 rad/s/div). (3) Stator phase current (100 A/div). (4) Rotor (DC excitation) current (10 A/div); time scale 500 ms/div [50].

TABLE I
"ACTIVE FLUX" CONCEPT: FUNDAMENTAL MODELS (FM)

Machine type	IPMSM	RSM	IM	Electrically Excited SM	F-M Machines
First proposals	Extended emf [1], 2000 Fictitious PM flux [7] 2005 Active Flux [8], 2008	Active flux [8] 2007			
Subsequent proposals	With SM or disturbance observers, [2], [11] [12—33] [58—63]	[35—43] [59]	NA	[50-51]	NA
Position speed observer	Robustness of active-flux sensorless control [65], [66], [68]	[22], [39], [41], [58]	[2] [10], [19], [24]	NA	NA
MTPA	[44], [64]	[45], [48]	NA	NA	NA
Scalar Control	[46]	[49]	[47]	NA	NA
MTPA Maxcosφ MTPF	NA	[45]	NA	NA	NA

The generic control scheme is shown in Fig. 9.

No other work (besides [51], [52]) on "active flux" control of electrically excited synchronous motors was found so far in the mainstream literature.

SI encoderless control with "active flux" will now be presented.

C. "Signal Injection" With "Active Flux"

As pointed out in the Introduction, basically "active flux" is aligned to d-axis in a machine with physical d–q saliency even at standstill and thus it is able to estimate rotor position by SI, too. An early implementation of "active flux" for an ALA—RSM encoderless control from zero speed [53] that already integrates SI (but still with injected current processing for rotor position) with "active flux" FOC, offering zero to 3000 r/min operation, is presented in [53].

In a more recent implementation for RSM [54] it was proved that by using a fundamental "active flux observer" for rotor position but processing q-axis flux for SI, zero speed operation is improved (smaller position error) in comparison with the injected current processing.

Pescetto et al. [55] is dedicated to SI by "active flux" in an RSM as it is applied only at standstill and small speeds, but it considers the magnetic saturation via transient inductances L_{dd}, L_{qq} while neglecting cross-coupling saturation.

It needed a LUT table of magnetization curves, but the results at standstill are outstanding (see Fig. 10).

D. Discussion on State of the Art

1) Tables I and II summarize the mainstream literature on "active flux" so far.

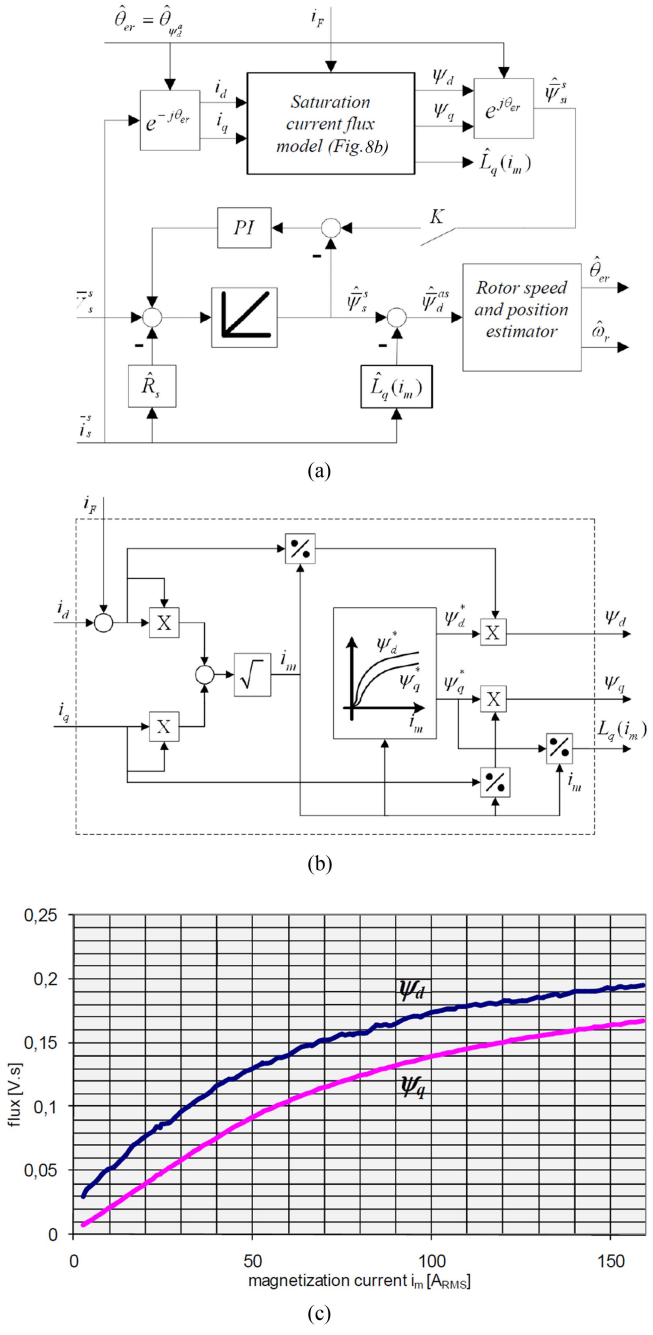

Fig. 8. Complete "active flux" plus cross-coupling saturation flux model of DC excited SM, for encoderless control: a) complete active flux observer, b) cross-coupling saturation flux model marked in a), and c) experimental on-line equivalent unique magnetization curves $\Psi_d^*(I_m)$, $\Psi_q^*(I_m)$, $I_m = \sqrt{(i_d + i_F)^2 + i_q^2}$, [50].

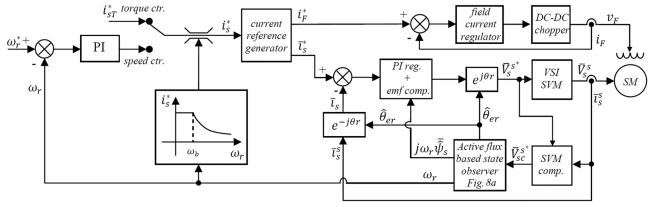

Fig. 9. Encoderless DC excited SM FOC with active flux observer, [53].

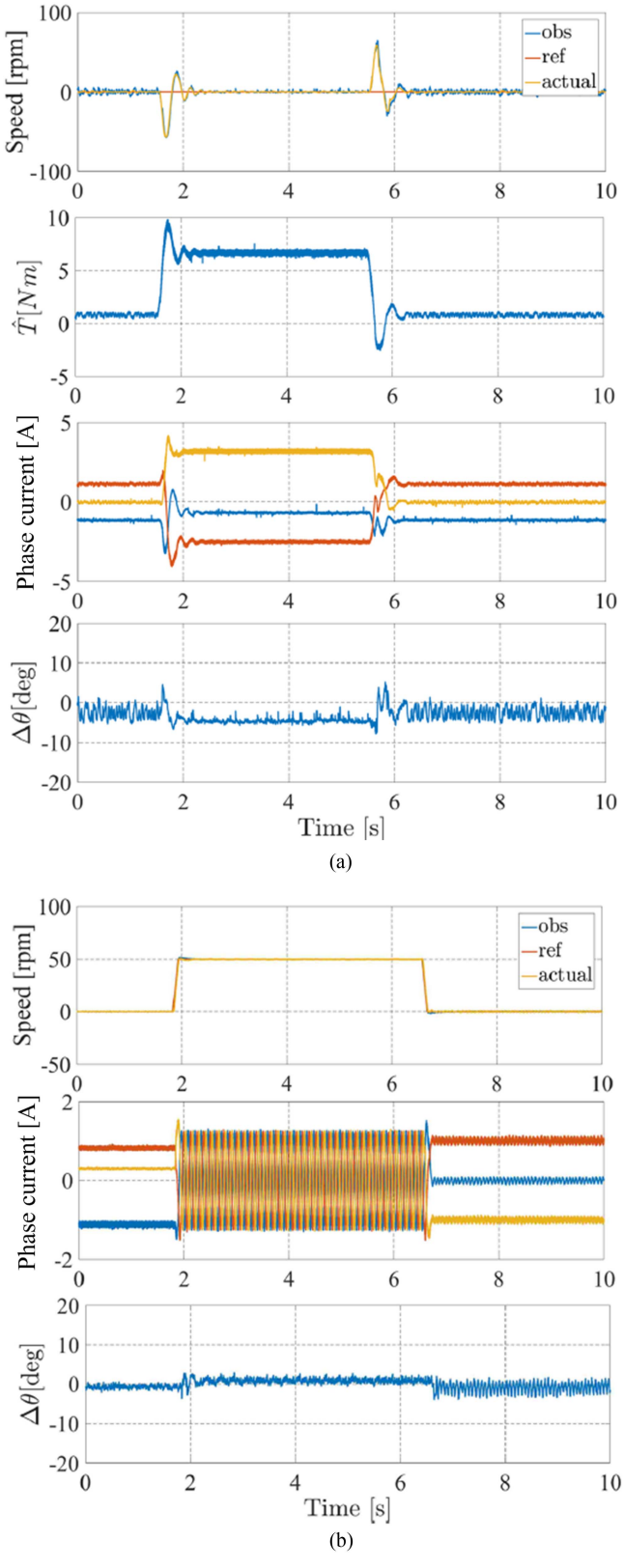

Fig. 10. Active flux SI encoderless RSM speed control test. (a) At standstill with step full loading and (b) no-load acceleration/deceleration to/from 50 r/min [55].

TABLE II
"ACTIVE FLUX" CONCEPT: SIGNAL INJECTION (SI) PLUS INTEGRATED SIGNAL INJECTION AND FUNDAMENTAL MODEL (SI+FM)

Machine type	IPMSM	RSM	IM	DC Excited SM	F-M Machines
First proposals	NA	[53], [54], [55], [67]	NA	NA	NA

2) The active flux, proved to be a phenomenological (physical) concept based on the simple formula: $\bar{\Psi}_d^a = \bar{\Psi}_s - \bar{I}_s L_q$, valid in any system of coordinates and aligned to rotor *d*-axis (for SMs, and, in principle to flux-modulation machines) and to rotor flux axis in IMs.
3) The "active flux" concept was applied in a unified manner for all synchronous and induction motor drives with notable performance in encoderless control with rather precise and robust (after correction for magnetic saturation) response (mainly using closed loop voltage plus current model and sliding mode "active flux" observers);
4) So far mainly the fundamental "active flux" model was particularly investigated for IPMSMs and RSMs and less for IMs and dc excited SMs and not yet for flux-modulation (F–M) machine drives [9].
5) Among the "active flux" observers the voltage—current closed loop (PI+SM) observer with PLL or with active disturbance compensation has been proven adequate for the scope: though other observers with disturbance estimation components may be suitable for same scope.
6) Despite of efforts, so far, to use SI, for heavy starts and prolonged 1–5 r/min operation, fusing "active flux" both for SI and fundamental model, considering cross-coupling saturation, is yet due;
7) Only a few very recent attempts have been made to use "active flux" also to simplify MTPA, MaxCosFi, MTPF, all fused smoothly for optimal operation for the entire torque-speed envelope of ac drives.

The next paragraph discusses such an endeavor.

III. "ACTIVE FLUX" FOR MTPA, MAXCOSFI, AND MTPF, IN AC DRIVES

A. Magnetic Saturation is Considered Constant

MTPA in synchronous (IPMSMs plus RSMs) has been investigated thoroughly by a multitude of methodologies [56], to reduce losses at given speed-torque operation modes when the required stator voltage is smaller than the maximum value available from the inverter, with, in general, a smooth passing to MTPF (is required).

As long as overmodulation is available and then for six pulse operation, rather reconfigurable control is required especially for wide CPSR as in electric power trains.

While widely accepted in theory, a full torque—speed envelope control for low losses in the electric machine drives observing both stator current and voltage limitations is still due.

Here, aiming at such a goal, we first describe as an alternative the use of "active flux" for integrated MTPA, MaxCosFi, and MTPF control in ac machine drives, first considering a constant magnetic saturation in the machine.

Note: In general, MTPA and MTPF are used in the literature as fused operation modes to optimize the entire torque-speed range in ac drives. Here we add in between (especially for RSM, IM, and wide CPSR IPMSM drives) the max ideal power factor mode because it leads to higher torque (for same stator flux) and given speed and voltage and because it is also weakly dependent on speed. In contrast to efficiency, though losses increase actual power factor in motoring and reduce it in generating mode.

It should be mentioned that MTPA for IPMSMs may be used up to full (max.) torque and up to base speed, while for RSMs (or IMs) going towards MaxCosFi will produce more torque for a given voltage with high saliency: L_d/L_q (RSM) or L_s/L_{sc} (IM).

In what follows we will derive the conditions for MTPA, MaxCosFi, MTPF directly for IPMSM; RSM and IM are particular cases with $\Psi_{F0} = 0$; magnetic saturation is still considered constant.

a) Existing MTPA [44]: For a given torque, based on the active flux expression (3) the stator current of IPMSM i_s (peak phase value) is

$$i_s^2\left(\Psi_d^a\right) = \left(\frac{\left(\Psi_d^a - \Psi_F\right)}{L_d - L_q}\right)^2 + \left(\frac{2T_e^*}{3p_1\Psi_d^a}\right)^2 < i_{s\max}^2. \quad (9)$$

By making the derivative of (9) with respect to Ψ_d^a (active flux) zero, for given reference torque T_e^*, we obtain simply [44]

$$\left(\Psi_d^a\right)^4 - \left(\Psi_d^a\right)^3\Psi_F - \left(\frac{2T_e^*}{3p_1}\left(L_d - L_q\right)\right)^2 = 0. \quad (10)$$

With $\Psi_F = L_{dm}i_F^*$ for dc excited SM; $\Psi_F = \Psi_{\mathrm{PM}d}$ for IPMSMs and $\Psi_F = 0$ for RSM (for IM also, $L_d \to L_s$, $L_q \to L_{sc}$).

Equation (10) was solved in [44] in 4-5 iterations (by Newton–Raphson method) online for IPMSMs

$$\Psi_d^a(k) = \Psi_d^a(k-1) - \frac{\left(\Psi_d^a(k-1)\right)^4 - \left(\Psi_d^a(k-1)\right)^3\Psi_{PMd} - \left(\frac{2T_e^*}{3p_1}\left(L_d - L_q\right)\right)^2}{4\left(\Psi_d^a(k-1)\right)^3 - 3\left(\Psi_d^a(k-1)\right)^2\Psi_{\mathrm{PM}d}}. \quad (11)$$

More than 10% stator current reduction, with respect to conventional methodologies has been reported experimentally [44].

b) Proposed MTPF: This time simply we express Ψ_s^2 as a function of Ψ_d^a

$$\Psi_s^2\left(\Psi_d^a\right) = \left(\Psi_F + \frac{L_d\left(\Psi_d^a - \Psi_F\right)}{L_d - L_q}\right)^2 + \left(\frac{2T_e^*L_q}{3p_1\Psi_d^a}\right)^2 < V_{s\max}^2/\omega_r^2. \quad (12)$$

Making the derivative of (12) with respect to Ψ_d^a zero we obtain

$$\left(\Psi_d^a\right)^4 - \left(\Psi_d^a\right)^3\left(1 - \frac{\left(L_d - L_q\right)}{L_d}\right)\Psi_F$$

$$-\left(\frac{2T_e^*}{3p_1}\left(L_d-L_q\right)\frac{L_q}{L_d}\right)^2=0. \tag{13}$$

An iterative solution of (13) may be obtained similarly as done in (11).

c) Proposed MaxCosFi: Here we use $\tan\varphi$ (φ – power factor angle):

$$\tan\varphi\left(\Psi_d^a\right)=\frac{\Psi_d i_q-\Psi_q i_d}{\Psi_d i_d+\Psi_q i_q}$$

$$=\frac{T_e^*\frac{2}{3p_1}}{\Psi_d^a\frac{\left(\Psi_d^a-\Psi_F\right)}{L_d-L_q}+L_d\left(\frac{\left(\Psi_d^a-\Psi_F\right)}{L_d-L_q}\right)^2+\left(\frac{2T_e^*}{3p_1\Psi_d^a}\right)^2}. \tag{14}$$

Zeroing the derivative of (14) with respect to Ψ_d^a we obtain

$$\left(\Psi_d^a\right)^4-\left(\Psi_d^a\right)^3\Psi_F\left(1-\frac{\left(L_d-L_q\right)}{2L_d}\right)$$

$$-\left(\frac{3T_e^*}{3p_1}\left(L_d-L_q\right)\right)^2\frac{L_q}{L_d}=0. \tag{15}$$

Note: It could be simply proven that for given torque the minimum stator flux Ψ_s (12) (minimum stator voltage for given speed) is obtained for MTPF, then for MaxCosFi and, then max Ψ_s for MTPA

$$\left(\Psi_s\right)_{T_e^*}^{\text{MTPA}}>\left(\Psi_s\right)_{T_e^*}^{\text{MaxCosFi}}>\left(\Psi_s\right)_{T_e^*}^{\text{MTPF}}. \tag{16}$$

Consequently, it is sufficient to post calculate the voltage $V_s^*\approx\omega_r\Psi_s^*$ [with Ψ_s^* from (12) for given T_e^* and speed and Ψ_d^a from (10), (13), and (15)] and to use the control strategy that leads to $V_s\le V_s^*$. If two of them satisfy the condition the one with minimum total electric losses will be applied

$$\sum p=\frac{3}{2}R_s i_s^2+\frac{3}{2}R_r i_r^2+k_{\text{iron}}V_s^2 \tag{17}$$

where the core losses are considered simply proportional to V_s^2, which covers approximately for the harmonic core losses as it considers all core losses to be eddy current losses. For a single given Ψ_s and ω_1 the core losses have to be known, in order to determine approximately the coefficient k_{iron}.

For the RSM (10), (13), (15) get simplified (as $\Psi_{F0}=0$)

$$\left(\Psi_d^a\right)_{\text{MTPA}}=\sqrt{\frac{2\left|T_e^*\right|}{3p_1}\left(L_d-L_q\right)}$$

$$\left(\Psi_d^a\right)_{\text{Maxcos}\varphi}=\left(\Psi_d^a\right)_{MTPA}\sqrt[4]{\frac{L_q}{L_d}}$$

$$\left(\Psi_d^a\right)_{\text{MTPF}}=\left(\Psi_d^a\right)_{MTPA}\sqrt{\frac{L_q}{L_d}}. \tag{18}$$

Note: For IMs basically, (18) is valid with $L_d\to L_s$, $L_q\to L_{\text{sc}}$; $\frac{L_q}{L_d}<1$ and $\frac{L_{sc}}{L_s}<<1$.

For dc excited SMs it is possible to repeat the calculation above for a few values of field current and choose the desired control strategy. However, for more precision, a direct derivation of MTPA, MaxCosFi = 1 and MTPF conditions is recommended for such a case.

TABLE III
ALA ROTOR SYNREL PARAMETERS

Parameter	Value
Rated power	157 W
Number of pole pairs	$p=2$
Stator phase resistance	$R=0.61\ \Omega$
Drive dc-link voltage	$V_{\text{dc}}=48$ V
Rated frequency	$f_n=50$ Hz
Rated speed	$n_n=1500$ r/min
Rated phase current	5.2 A
Inertia of rotor	$J=1\text{x}10\text{-}3$ Kg m^2
Viscous friction coefficient	$B=0.7\text{x}10\text{-}3$ N·ms/rad

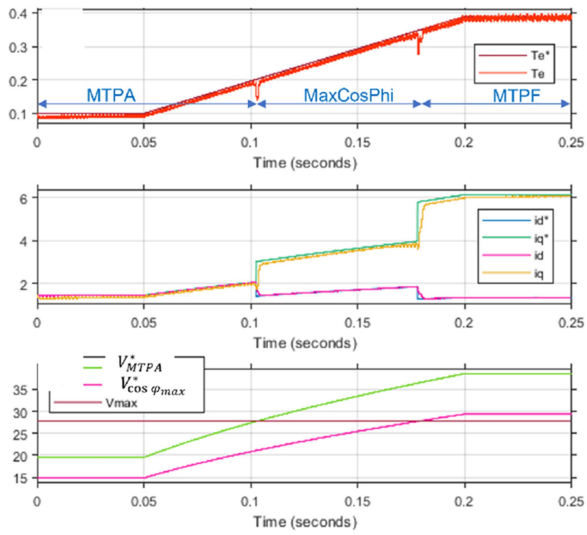

Fig. 11. ALA rotor RSM – MTPA + Maxcosφ + MTPF "active flux": simulation results at 3000 r/min.

B. An RSM Case Study

In [45], the integrated MTPA—MaxCosFi—MTPF control strategies have been applied on an ALA RSM (see Table III) with rather smooth transitions and promising results for the entire torque and speed range, but still with constant machine parameters.

Sample results from [45] are given in Figs. 11 and 12.

The simulation results in Fig. 11 prove that the successful transition between the three strategies that cover all torque–speed range is rather smooth (stable, too) and that the max. available voltage is observed (see Fig. 12). Experiments (see Fig. 12) confirm rather satisfactorily the simulation results.

From Fig. 13 we retained average linear curves of d- and q-axes measured flux linkages.

However, tempting as they are, the above simplifications by using "active flux" for MTPA—MaxCosFi—MTPF for all ac drives in absence of magnetic saturation variation, the consideration of the latter has to be thoroughly investigated too. This is done in the following paragraph.

C. Proposed Magnetic Saturation as Accounted for via "Active Flux" for all AC Drives

The key to a simplified version of considering magnetic saturation is to assume $L_q=\text{const}$, but L_d as a given function of active

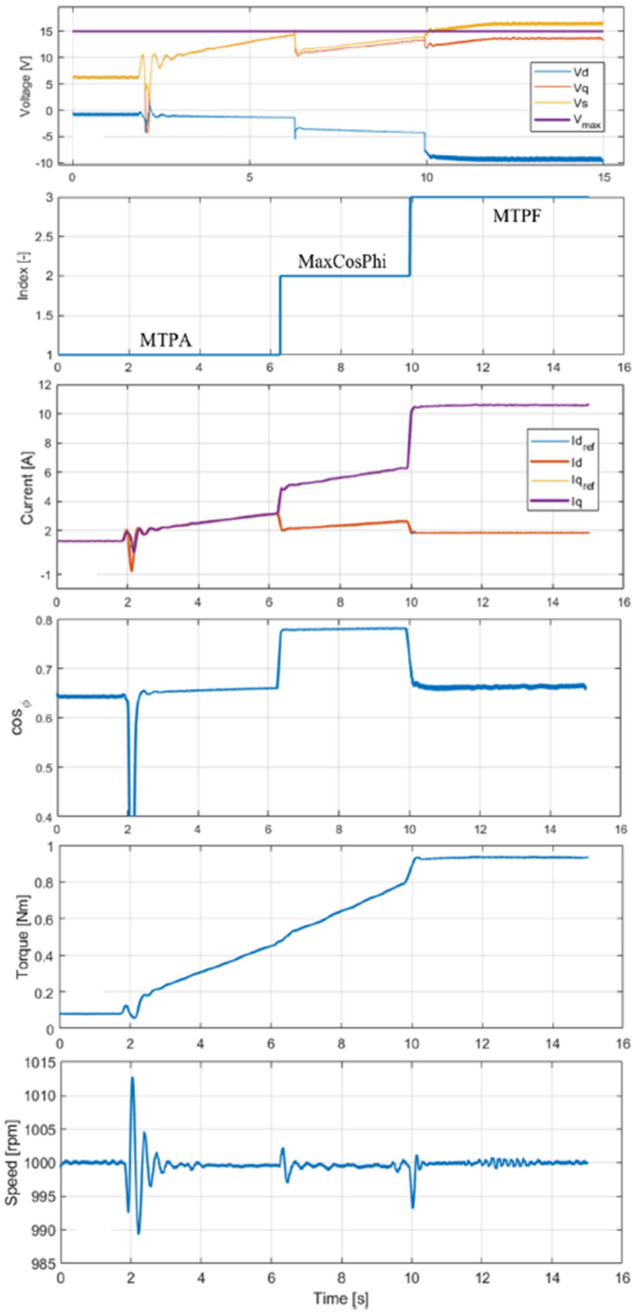

Fig. 12. ALA rotor RSM – MTPA + Maxcosφ + MTPF "active flux" control: experimental test results at 1000 r/min [45].

flux $L_d(\ \Psi_d^a\ )$, thus neglecting the cross-coupling saturation. Consequently, we simply restart from (9), (12), and (14) but in the zeroing of their derivatives with respect to Ψ_d^a we will consider now that L_d is $L_d(\ \Psi_d^a\ )$, to obtain finally.

For MTPA

$$-\frac{\frac{\partial L_d}{\partial \Psi_d^a}}{(-L_q)^3}\left(\Psi_d^a-\Psi_{F0}\right)^2+\frac{\left(\Psi_d^a-\Psi_{F0}\right)}{\left(L_d\left(\Psi_d^a\right)-L_q\right)^2}-\left(\frac{2T_e^*}{3p_1}\right)^2\frac{1}{\left(\Psi_d^a\right)^3}=0. \tag{19}$$

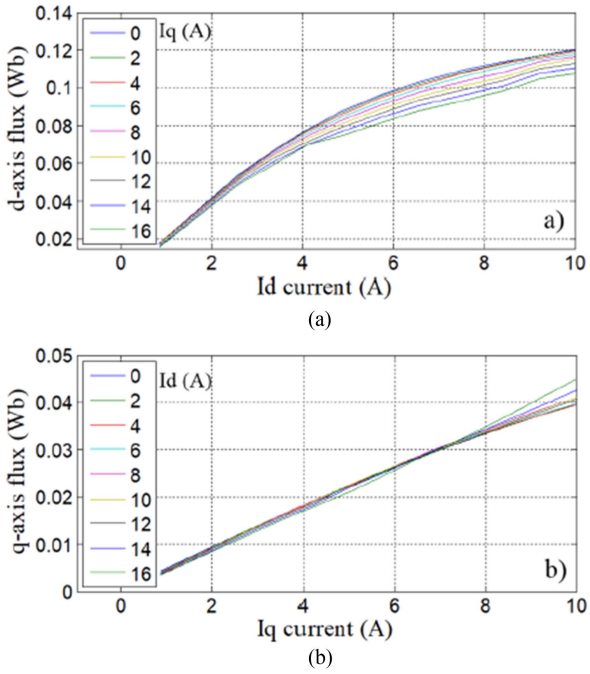

Fig. 13. Magnetization curves of the motor in Table III. (a) d- axis (b) q-axis.

For MaxCosFi

$$-L_d\left(\Psi_d^a\right)\cdot\frac{\partial L_d}{\partial \Psi_d^a}\cdot\frac{\left(\Psi_d^a-\Psi_{F0}\right)^2\cdot L_q}{\left(L_d\left(\Psi_d^a\right)-L_{q0}\right)^3}+\frac{\Psi_d^a\cdot L_d^2\left(\Psi_d^a\right)}{\left(L_d\left(\Psi_d^a\right)-L_{q0}\right)^2}-\left(\frac{2T_e^*L_q}{3p_1}\right)^2\frac{1}{\left(\Psi_d^a\right)^3}=0. \tag{20}$$

For MTPF

$$-\frac{\partial L_d}{\partial \Psi_d^a}\cdot\frac{\left(\Psi_d^a-\Psi_{F0}\right)^2}{\left(L_d\left(\Psi_d^a\right)-L_{q0}\right)^3}\left(L_d\left(\Psi_d^a\right)+L_q\right)+\frac{2\cdot\left(\Psi_d^a-\Psi_{F0}\right)\cdot L_d\left(\Psi_d^a\right)}{\left(L_d\left(\Psi_d^a\right)-L_{q0}\right)^2}-\left(\frac{2T_e^*}{3p_1}\right)^2\cdot\frac{2L_{q0}}{\left(\Psi_d^a\right)^3}=0. \tag{21}$$

The apparently complex (19)–(21) may be solved in a few iterations by the Newton–Raphson method [as (11)] [44]. Ψ_{F0} and L_{q0} mark the fact that these parameters are considered constant.

Note: Identifying $L_d(\ \Psi_d^a\ )$ is "a fruit" of $|\widehat{\Psi}_d^a|=\Psi_{F0}+(L_d-L_q)i_{d0}$ which is the amplitude of $|\widehat{\Psi}_d^a|$ obtained already in the $\widehat{\Psi}_d^a$ observer, but not used so far in the literature. With Ψ_{F0}, L_q given and i_d known from the FOC diagram, we may invert the above equation point by point to get the $L_d(\ \Psi_d^a\ )$ function.

A very recent paper includes magnetic saturation for direct active flux and torque deadbeat control for flux weakening and max. torque up to base speed with stator resistance voltage drop consideration [64].

IV. Final Discussions and Conclusion

1) "Active flux" concept $\Psi_d^a = \Psi_{Fd} + (L_d - L_q)i_d$ has been introduced for all ac machines as a generalization in 2008, of "virtual PM flux" derived, only for IPMSM [7], in 2005.
2) "Active flux" is a technical concept representing an equivalent ac machine without functional saliency while the original ac machine may have saliency (physical or virtual (IM)).
3) The "active flux" space phasor of ac machines (traveling field and flux-modulation types) is ideally (with constant machine parameters) aligned to axis d of all synchronous and F–M machines and along the rotor flux in IMs and shows only the inductance *Lq*.
4) The "active flux" may be applied also along axis q $\Psi_q^a = \Psi_{Fq} + (L_q - L_d)i_q$ when the model will show, again, only one inductance: *Ld* [35].
5) Being aligned to the rotor d axis for correct machine parameters, in SMs and F-M machines with physical saliency and fractional in any system of coordinates (at any speed), "active flux" simplifies the rotor position estimation in encoderless drives. So "active flux" may be used not only as "fundamental active flux" but also in "SI active flux" observers, avoiding the low-speed large errors by SOGI variants or by adaptive robust disturbance observers integrated with "active flux" close loop voltage plus current model PI or PI+SM observers.
6) As of now, "active flux" has been implemented very recently in better and better configurations for encoderless IPMSM and RSM drives, including stator resistance adaptation [65], [66], a new combined active flux with SI control from zero to maximum speed [67] and compensation of inverter nonlinearity voltage errors [68].
7) However, Tables I and II showed many "NA" positions, so there is still a lot of work to do.

In order to improve the technology, the following may be considered.

1) Even better, more robust and more precise "active flux" observers for the entire speed-torque range in various applications
2) MTPA+MaxCosFi+MTPF full torque-speed envelope control, observing the limited current and voltage of the inverter, by applying "active flux;" a draft theory of such an endavor is included in this article without and with considering magnetic saturation variation with torque and speed.
3) Novel, "active flux" based, self-commissioning schemes for all ac encoderless drives.
4) "Active flux" based encoderless control of electric generators in wind energy and marine slip power systems
5) Extension of "active flux" control to dc excited SM drives for e-transport; and to F–M machine drives
6) Potential generalization of "active flux" usage in scalar control and also model predictive control of ac drives.

We should end, in a note of humbleness since "active flux" concept is just one potentially useful/practical alternative for better control of unified ac motor/generator drives and not "the one that solves it all."

REFERENCES

[1] Z. Chen, M. Tomita, S. Ichikawa, S. Doki, and S. Okuma, "Sensorless control of interior permanent magnet synchronous motor by estimation of an extended electromotive force," in *Proc. Conf. Rec. IEEE Ind. Appl. Conf. 35th IAS Annu. Meeting World Conf. Ind. Appl. Elect. Energy*, 2000, pp. 1814–1819.

[2] J. Chen, Xin Yuan, Frede Blaabjerg, and C. H. T. Lee, "Overview of fundamental frequency sensorless algorithms for AC Motors: A unified perspective," *IEEE-JESTPE*, vol. 11, no. 1, pp. 915–931, 2023.

[3] C. Lascu, I. Boldea, and F. Blaabjerg, "Direct torque control of sensorless induction motor drives a sliding-mode approach," *IEEE Trans. Ind. Appl.*, vol. 40, no. 2, pp. 582–590, Mar./Apr. 2004.

[4] C. Lascu, I. Boldea, and F. Blaabjerg, "Direct torque control via feedback linearization for permanent magnet synchronous motor drives," in *Proc. 13th Int. Conf. Optim. Elect. Electron. Equip.*, 2012, pp. 338–343.

[5] N.-D. Nguyen, N. N. Nam, C. Yoon, and Y. Il Lee, "Speed sensorless model predictive torque control of induction motors using a modified adaptive full-order observer," *IEEE Trans. Ind. Electron.*, vol. 69, no. 6, pp. 6162–6172, Jun. 2022.

[6] R. Sreejith and B. Singh, "Sensorless predictive current control of PMSM EV drive using DSOGI-FLL based sliding mode observer," *IEEE Trans. Ind. Electron.*, vol. 68, no. 7, pp. 5537–5547, Jul. 2021.

[7] S. Koonlaboon and S. Sangwongwanich, "Sensorless control of interior permanent-magnet synchronous motors based on a fictitious permanent-magnet flux model," in *Proc. 40th IAS Annu. Meeting. Conf. Rec. 2005 Ind. Appl. Conf.*, 2005, pp. 311–318.

[8] I. Boldea, M. C. Paicu, and G.-D. Andreescu, "Active flux concept for motion-sensorless unified AC drives," *IEEE Trans. Power Electron.*, vol. 23, no. 5, pp. 2612–2618, Sep. 2008.

[9] I. Boldea and L. Tutelea, *Reluctance Electric Machine Design and Control*. Boca Raton, FL, USA: CRC Press, 2021.

[10] S. Zhou et al., "A robust encoderless control for PMSM drives: A revised hybrid active flux-based technique," *IEEE Trans. Power Electron.*, vol. 38, no. 11, pp. 14438–14449, Nov. 2023.

[11] I. Boldea and S. C. Agarlita, "The active flux concept for motion-sensorless unified AC drives: A review," in *Proc. Int. Aegean Conf. Elect. Machines Power Electron. Electromotion, Joint Conf.*, 2011, pp. 1–16.

[12] M. C. Paicu, I. Boldea, and G. D. Andreescu, and F. Blaabjerg, "Very low speed performance of active flux based sensorless control: Interior permanent magnet synchronous motor vector control versus direct torque and flux control," *Proc. IET*, vol. 3, no. 6, pp. 551–561, 2009.

[13] M. Koteich, G. Duc, A. Maloum, and G. Sandou, "A unified model for low-cost high-performance AC drives: The equivalent flux concept," in *Proc. 3rd Int. Conf. Elect., Electron., Comput. Eng. Appl.*, 2016, pp. 71–76.

[14] D. O. Kisck, D. S. Anghel, and M. Kisck, "Rotor-flux model for sensorless vector-control of super-high-speed IPMSM," in *Proc. 10th Int. Symp. Adv. Topics Elect. Eng.*, 2017, pp. 132–137.

[15] D. O. Kisck, M. Kisck, and D. S. Anghel, "Sensorless control of high-speed IPMSM based on rotor-flux and fictitious-flux estimation," in *Proc. IEEE Int. Elect. Machines Drives Conf.*, 2017, pp. 1–8.

[16] A. Varatharajan, G. Pellegrino, and E. Armando, "Sensorless synchronous reluctance motor drives: Auxiliary flux-based position observer," *IEEE-JESTPE*, vol. 9, no. 4, pp. 4330–4339, 2021.

[17] M. Mamdouh, S. M. Ismaeel, S. M. Allam, and E. M. Rashad, "A proposed active flux based sensorless control of cage-rotor synchronous reluctance motor," in *Proc. 22nd Int. Middle East Power Syst. Conf.*, 2021, pp. 449–454.

[18] M. Costin and C. Lazar, "Active flux based predictive control of interior permanent magnet synchronous machine," in *Proc. Int. Symp. Fundamentals Elect. Eng.*, 2020, pp. 1–6.

[19] Q. Lin, L. Liu, and D. Liang, "Hybrid active flux observer to suppress position estimation error for sensorless IPMSM drives," *IEEE Trans. Power Electron.*, vol. 38, no. 1, pp. 872–886, Jan. 2023.

[20] A. Ejlali, S. Taravat, and J. Soleimani, "Comparative study on control strategy of DTFC based on active flux concept and DTC for IPMSM applied to traction motor," in *Proc. Int. Symp. Power Electron. Power Electron., Elect. Drives, Automat. Motion*, 2012, pp. 200–206.

[21] S. M. S. Islam Shakib, D. Xiao, R. Dutta, and M. F. Rahman, "Online deadbeat predictive control for IPMSM drive," in *Proc. Int. Power Electron. Conf.*, 2022, pp. 2479–2483.

[22] Y.-Ch. Liu, S. Laghrouche, A. N'Diaye, and M. Cirrincione, "Active-flux-based super-twisting sliding mode observer for sensorless vector control of synchronous reluctance motor drives," in *Proc. 7th Int. Conf. Renew. Energy Res. Appl.*, 2018, pp. 1–7.

[23] I. Boldea, M. C. Paicu, G.-D. Andreescu, and F. Blaabjerg, "Active flux" DTFC-SVM sensorless control of IPMSM," *IEEE Trans. Energy Convers.*, vol. 24, no. 2, pp. 314–322, Jun. 2009.

[24] A. T. Woldegiorgis, X. Ge, and M. Hassan, "Advanced disturbance observer-based active flux estimation for sensorless control of IPMSM," in *Proc. 10th Int. Conf. Power Electron., Machines Drives*, 2020, pp. 230–235.

[25] M. Zhang, C. Wu, and H. Xiao, "Second-sliding mode adaptive active flux control for interior permanent magnet synchronous motor," in *Proc. 2nd Int. Conf. Intell. Comput. Hum.-Comput. Interaction*, 2021, pp. 330–333.

[26] Z. Guoqiang, W. Gaolin, Ni Ronggang, and X. Dianguo, "Active flux based full-order discrete-time sliding mode observer for position sensorless IPMSM drives," in *Proc.17th Int. Conf. Elect. Machines Syst.*, 2014, pp. 3569–3572.

[27] K. Zhao, R. Zhou, J. She, and P. Li, "Active – flux – based sensorless control for permanent magnet synchronous motor by variable – gain sliding – mode observer," in *Proc. IEEE 16th Int. Conf. Control Automat.*, 2020, pp. 1559–1564.

[28] M.-C. Ancuti, A.-S. Isfanuti, G.-D. Andreescu, L.-N. Tutelea, and I. Boldea, "Referencing position versus speed active flux based encoderless control of PM-RSM drives at ultra-low speeds without signal injection," in *Proc. Int. Aegean Conf. Elect. Machines Power Electron.*, 2021, pp. 159–166.

[29] A. Ejlali, D. A. Khaburi, and H. Behnia, "DTFC based indirect matrix converter using active flux concept for IPMSM drive," in *Proc. 46th Int. Universities' Power Eng. Conf.*, 2011, pp. 1–4.

[30] C. R. S. Bartsch, L. F. F. de Campos, A. G. Bartsch, J. de Oliveira, and A. Nied, "Low computational cost technique for SPMSM sensorless drive using active flux concept," in *Proc. IEEE Proc. 15th Braz. Power Electron. Conf., 5th IEEE Southern Power Electron. Conf.*, 2019, pp. 1–6.

[31] W. Liu, S. G. Ding, Y. H. Dong, H. Jin, K. Huang, and Z. W. Hu, "Sensorless control strategy for IPMSM based on ADRC and differential of active flux," in *Proc. IEEE 9th Int. Conf. Electron. Inf. Emerg. Commun.*, 2019, pp. 1–5.

[32] A. T. Woldegiorgis, X. Ge, H. Wang, and M. Hassan, "A new frequency adaptive second-order disturbance observer for sensorless vector control of interior permanent magnet synchronous motor," *IEEE Trans. Ind. Electron.*, vol. 68, no. 12, pp. 11847–11857, Dec. 2021.

[33] F. Toso, P. G. Carlet, M. Preindl, and S. Bolognani, "Active-flux-based motion-sensorless control of PMSM using moving horizon estimator," in *Proc. IEEE 9th Int. Symp. Sensorless Control Elect. Drives*, 2018, pp. 78–83.

[34] S.-C. Agarliţă, M. Fătu, L. N. Tutelea, F. Blaabjerg, and I. Boldea, "I-f starting and active flux based sensorless vector control of reluctance synchronous motors, with experiments," in *Proc. 12th Int. Conf. Optim. Elect. Electron. Equip.*, 2010, pp. 337–342.

[35] Z. Zhang and J. Lamb, "Active Q flux concept for sensorless control of synchronous reluctance machines," *IEEE Trans. Ind. Electron.*, vol. 70, no. 5, pp. 4526–4536, May 2023.

[36] H. Hadla and S. Cruz, "Active flux based finite control set model predictive control of synchronous reluctance motor drives," in *Proc. Eur. Conf. Power Electron. Appl.*, 2016, pp. 1–10.

[37] F. J. W. Barnard, W. Villet, and M. Kamper, "Hybrid active-flux and arbitrary injection position sensorless control of reluctance synchronous machines," *IEEE Trans. Ind. Appl.*, vol. 51, no. 5, pp. 3899–3906, Sep./Oct. 2015.

[38] B. Zhenfeng, W. Sun, and D. Jiang, "Speed sensorless control of synchronous reluctance motor at full speed range," in *Proc. IEEE 4th Int. Elect. Energy Conf.*, 2021, pp. 1–5.

[39] A. Varatharajan and G. Pellegrino, "Sensorless synchronous reluctance motor drives: A projection vector approach for stator resistance immunity and parameter adaptation," *IEEE Trans. Ind. Appl.*, vol. 56, no. 5, pp. 5003–5012, Sep./Oct. 2020.

[40] B. Nikmaram and H. Pairo, "Comparison study of active flux based sliding-mode observer and PLL based sliding-mode observer sensorless control of SynRM," in *Proc. 12th Power Electron., Drive Syst., Technol. Conf.*, 2021, pp. 1–7.

[41] A. Varatharajan and G. Pellegrino, "Sensorless control of synchronous reluctance motor drives: Improved modeling and analysis beyond active flux," in *Proc. IEEE Int. Elect. Machines Drives Conf.*, 2019, pp. 419–426.

[42] J. Matoušek, J. Duník, M. Brandner, and V. Elvira, "Comparison of discrete and continuous state estimation with focus on active flux scheme," in *Proc. 24th Int. Conf. Inf. Fusion*, 2021, pp. 1–8.

[43] N. Bianchi, S. Bolognani, F. Tinazzi, and M. Zigliotto, "The influence of rotor design on active flux-based sensorless synchronous reluctance motor drives," in *Proc. IEEE Int. Symp. Sensorless Control Elect. Drives*, 2017, pp. 7–12.

[44] S. Liu, W. Huang, X. Lin, Y. Zhao, W. Jiang, and J. Yang, "Maximum torque per ampere control based on active flux concept for DTC of IPMSMs," in *Proc. IEEE Energy Convers. Congr. Expo.*, 2018, pp. 6558–6562.

[45] S. C. Agarlita, A. S. Isfanuti, and I. Boldea, "Active flux based control of ALA Rotor SynRel with MTPA, maximum power factor and maximum torque per flux," in *Proc. Int. Aegean Conf. Elect. Machines Power Electron., 2023 Int. Conf. Optim. Elect. Electron. Equip.*, 2023, pp. 1–6.

[46] A.-S. Isfanuti, M.-C. Paicu, L.-N. Tutelea, T. Staudt, and I. Boldea, "V/f with stabilizing loops versus FOC of Spoke-PM rotor SM drive: Control with experiments," in *Proc. IEEE 18th Int. Power Electron. Motion Control Conf.*, 2018, pp. 629–636.

[47] A. A. Popa, A. S. Isfanuti, L. N. Tutelea, and I. Boldea, "Induction machine V/f control with stator flux and slip frequency compensation for maximum power factor, with experiments," in *Proc. Int. Aegean Conf. Elect. Machines Power Electron., Int. Conf. Optim. Elect. Electron. Equip.*, 2023, pp. 1–6.

[48] M. Vidlak, S. C. Agarlita, and I. Boldea, "MTPA control strategy for ALA rotor RSM based on reactive and apparent power calculation," in *Proc. Int. Conf. Elect. Drives Power Electron.*, 2023, pp. 1–6.

[49] A. A. Popa, A. S. Isfanuti, L. N. Tutelea, and I. Boldea, "V/f with stabilizing loops fast response control of induction motor (IM) drives," in *Proc. Int. Aegean Conf. Elect. Machines Power Electron., Int. Conf. Optim. Elect. Electron. Equip.*, 2021, pp. 135–142.

[50] I. Boldea, G. D. Andreescu, C. Rossi, A. Pilati, and D. Casadei, "Active flux based motion-sensorless vector control of DC-excited synchronous machines," in *Proc. IEEE Energy Convers. Congr. Expo.*, 2009, pp. 2496–2503.

[51] V. Coroban-Schramel, I. Boldea, G.-D. Andreescu, and F. Blaabjerg, "Active-flux based motion sensorless vector control of biaxial excitation generator/motor for automobiles (BEGA)," *IEEE Trans. Ind. Appl.*, vol. 47, no. 2, pp. 812–819, Mar./Apr. 2011.

[52] I. Boldea and S. C. Agarlita, "The active flux concept for motion-sensorless unified AC drives: A review," in *Proc. Int. Aegean Conf. Elect. Machines Power Electron. Electromotion, Joint Conf.*, 2011, pp. 1–16.

[53] S. C. Agarlita, I. Boldea, and F. Blaabjerg, "High frequency injection assisted 'active flux' based sensorless vector control of reluctance synchronous motors, with experiments from zero speed," *IEEE Trans. Ind. Appl.*, vol. 48, no. 6, pp. 1931–1939, Nov./Dec. 2012.

[54] A. Y.-Talouki, P. Pescetto, G. Pellegrino, and I. Boldea, "Combined active flux and high-frequency injection methods for sensorless direct-flux vector control of synchronous reluctance machines," *IEEE Trans. Power Electron.*, vol. 33, no. 3, pp. 2447–2457, Mar. 2018.

[55] P. Pescetto, A. Y.-Talouki, and G. Pellegrino, "Novel sensorless control algorithm for SyR Machines based on low speed active flux," in *Proc. IEEE 10th Int. Symp. Sensorless Control Elect. Drives*, 2019, pp. 1–6.

[56] A. Dianov, F. Tinazzi, S. Calligaro, and S. Bolognani, "Review and classification of MTPA control algorithms for synchronous motors," *IEEE Trans. Power Electron.*, vol. 37, no. 4, pp. 3990–4007, Apr. 2022.

[57] A. T. Woldegiorgis, X. Ge, H. Wang, and Y. Zuo, "An active flux estimation in the estimated reference frame for sensorless control of IPMSM," *IEEE Trans. Power Electron.*, vol. 37, no. 8, pp. 9047–9060, Aug. 2022.

[58] F. Gao, Z. Yin, C. Bai, D. Yuan, and J. Liu, "A lag compensation-enhanced adaptive quasi-fading Kalman filter for sensorless control of synchronous reluctance motor," *IEEE Trans. Power Electron.*, vol. 37, no. 12, pp. 15322–15337, Dec. 2022.

[59] J. Chen, J. Mei, X. Yuan, Y. Zuo, J. Zhu, and C. H. T. Lee, "Online adaptation of two-parameter inverter model in sensorless motor drives," *IEEE Trans. Ind. Electron.*, vol. 69, no. 10, pp. 9860–9871, Oct. 2022.

[60] Y. Li, Y. Hu, X. Ma, and L. Liu, "Sensorless control of dual three-phase IPMSM based on frequency adaptive linear extended state observer," *IEEE Trans. Power Electron.*, vol. 38, no. 11, pp. 14492–14503, Nov. 2023.

[61] F. Butaru, C. Carstea, A-I. Ratiu, M.-C. Ancuti, and S. Musuroi, "Active flux observer-based high-speed control of a permanent magnet synchronous motor," in *Proc. Rec. 13th Int. Symp. Adv. Topics Elect. Eng.*, 2023, pp. 1–5.

[62] A. Wang et al., "Two stage active flux observer for position sensorless control of PMSM drives," in *Proc. 26th Int. Conf. Elect. Machines Syst.*, 2023, pp. 5032–5037.

[63] M. Fontana and N. Bianchi, "Design and analysis of normal saliency IPM spoke motor," *IEEE Trans. Ind. Appl.*, vol. 56, no. 4, pp. 3625–3635, Jul./Aug. 2020.

[64] S M. Sh. I. Shakib, D. Xiao, R. Dutta, and M. F. Rahman, "An optimal maximum torque per active flux and field weakening operation for dead-beat direct torque control based IPMSM drive," *IEEE Trans. Ind. Appl.*, vol. 60, no. 2, pp. 3210–3220, Mar./Apr. 2024.

[65] S. Zhou et al., "A robust encoderless control for PMSM drives: A revised hybrid active flux-based technique," *IEEE Trans. Power Electron.*, vol. 38, no. 11, pp. 14438–14449, Nov. 2023.

[66] Q. Lin, L. Liu, and D. Liang, "Joint estimation of resistance and speed with auxiliary state of active flux for sensorless IPMSM drives," *IEEE Trans. Ind. Electron.*, vol. 66, no. 4, pp. 2659–2667, Apr. 2019.

[67] F. Lee, Z. Zhao, Y. Wang, and C. Shen, "Combined active flux and High-frequency injection methods for sensorless control of synchronous reluctance machines," in *Proc. IEEE 2nd Int. Power Electron. Appl. Symp.*, 2023, pp. 2332–2336.

[68] H. Li, S. Zhou, Z. Zhang, and Z. Li, "A hybrid active flux observer based encoderless control method for AC motor drives," in *Proc. 26th Int. Conf. Elect. Machines Syst.*, 2023, pp. 1–4.